

RESEARCH ARTICLE

A two-decade analysis of the spatial and temporal variations in burned areas across Zimbabwe

Munyaradzi Davis Shekede¹, Samuel Kusangaya^{1*}, Courage B. Chavava¹,
Isaiah Gwitira¹, Abel Chemura^{2,3}

1 Department of Geography Geospatial Sciences and Earth Observation, University of Zimbabwe, Harare, Zimbabwe, **2** Potsdam Institute for Climate Impact Research (PIK), Member of the Leibniz Association, Potsdam, Germany, **3** Department of Natural Resources, Faculty of Geo-Information Science and Earth Observation, University of Twente, Enschede, The Netherlands

* kusangayas@yahoo.com



Abstract

Understanding wildfire dynamics in space and over time is critical for wildfire control and management. In this study, fire data from European Space Agency (ESA) MODIS fire product (ESA/CCI/FireCCI/5_1) with $\geq 70\%$ confidence level was used to characterise spatial and temporal variation in fire frequency in Zimbabwe between 2001 and 2020. Results showed that burned area increased by 16% from 3,689 km² in 2001 to 6,130 km² in 2011 and decreased in subsequent years reaching its lowest in 2020 (1,161 km²). Over the 20-year period, an average of 40,086.56 km² of land was burned annually across the country. In addition, results of the regression analysis based on Generalised Linear Model illustrated that soil moisture, wind speed and temperature significantly explained variation in burned area. Moreover, the four-year lagged annual rainfall was positively related with burned area suggesting that some parts in the country (southern and western) are characterised by limited herbaceous production thereby increasing the time required for the accumulation of sufficient fuel load. The study identified major fire hotspots in Zimbabwe through the integration of remotely sensed fire data within a spatially analytical framework. This can provide useful insights into fire evolution which can be used to guide wildfire control and management in fire prone ecosystems. Moreover, resource allocation for fire management and mitigation can be optimised through targeting areas most affected by wildfires especially during the dry season where wildfire activity is at its peak.

OPEN ACCESS

Citation: Shekede MD, Kusangaya S, Chavava CB, Gwitira I, Chemura A (2024) A two-decade analysis of the spatial and temporal variations in burned areas across Zimbabwe. PLOS Clim 3(1): e0000201. <https://doi.org/10.1371/journal.pclm.0000201>

Editor: Alessandra Giannini, École Normale Supérieure: Ecole Normale Supérieure, FRANCE

Received: March 23, 2023

Accepted: December 2, 2023

Published: January 17, 2024

Copyright: © 2024 Shekede et al. This is an open access article distributed under the terms of the [Creative Commons Attribution License](https://creativecommons.org/licenses/by/4.0/), which permits unrestricted use, distribution, and reproduction in any medium, provided the original author and source are credited.

Data Availability Statement: All relevant data are within the paper and its [Supporting Information](#) files.

Funding: The authors received no specific funding for this work.

Competing interests: The authors have declared that no competing interests exist.

1. Introduction

In savanna ecosystems, fires are an important determinant for the co-existence of woody and herbaceous plants as they influence ecological processes such as tree-grass competition, grass productivity and tree recruitment [1]. Moreover, wildfires are critical in enabling nutrient cycling, seed germination and regulation of species composition and plant reproduction [2–5]. Previous studies have shown that a greater part of African savannas could transition to closed

woodlands under current climate in the absence of fire [6]. Wildfires also contribute significantly to greenhouse gas emissions and aerosols thereby making them an important driver of atmospheric radiative forcing and air quality [7]. Despite the importance of fires in controlling structure and function of ecosystems, elevated fire frequency and uncharacteristically extensive wildfires can result in biodiversity loss through destruction of plants and animals, reduction of soil fertility and increased soil erosion rates and decreased infiltration [8, 9].

Wildfires are driven by a myriad of factors such as human population increase, vegetation biomass production, temperature, humidity, wind speed and slope [10–12]. In savanna ecosystems, high vegetation production during the rainy season provides abundant fuel load for fires to occur and high temperatures during the dry season facilitate the spread of wildfires [3]. According to [8, 13] wildfires are also caused by anthropogenic activities such as hunting, using fire to improve grazing land, burning of crop residues, land preparation for farming and smoking out bees, unextinguished roadside fires used by travellers, and cigarettes butts improperly disposed. In addition to these, other human causes of wildfires are waste dumps and arson, but natural factors such as lightning can also cause fires [14].

According to [15], wildfires are a major cause of degradation in developing countries and 90% of the forest fires are ignited by human beings. Several studies have been carried out on wildfires in the savannas of Southern Africa [3, 14, 16–18]. Some of these studies focussed on drivers of wildfires, fire trends, fire frequency, burned area and fire hazard zones at districts or national level. Wildfires have caused extensive destruction to agricultural land, indigenous forests, national parks, rangelands, commercial timber plantations and communal grazing areas [8]. Thus, improved knowledge about the interaction between climate controls on the spatial and temporal variability in wildfire potential is needed for mitigating economic and other impacts of fires.

In general, many studies claimed that there was a significant increase in burned areas and coverage over the last years. However, all these studies were carried out at smaller spatial scales such as the district level and at comparatively short period of time, that which limits our understanding of wildfire patterns at large spatial and temporal scales [3, 16, 18]. Furthermore, these short time scales limit our ability to make conclusive statements about wildfire patterns [3]. Therefore, studies characterizing spatial and temporal wildfire patterns at large spatial and temporal scales could increase knowledge of wildfires thereby assisting responsible authorities to target wildfire hotspots and optimise distribution of limited resources efficiently. In addition, country-scale assessments are needed, that link biophysical climatic drivers to wildfire patterns that may suggest where mitigation steps can be taken to reduce economic threats to and ecological damage.

In recent years, the availability of satellite data has improved due to the increase in satellite missions in space which has enabled scholars to characterize wildfires at various spatial and temporal scales [3, 10, 19, 20]. Such sensors include Advanced Very High-Resolution Radiometer (AVHRR), Moderate Resolution Imaging Spectroradiometer (MODIS) and Landsat. These are long-term remote sensing systems with extensive image archives with improved calibration and recalibration for monitoring fire history and impacts over time. Furthermore, various global fire products that are now freely available have been applied to study numerous aspects of wildfires. These include the MODIS Burned Area Products MCD45A1 and MCD64A1, Medium Resolution Imaging Spectrometer (MERIS) Fire CCI Products, Copernicus Burned Area Products and the GLOBCARBON product [21]. Before the advent of satellites, it was difficult and, time consuming to characterize wildfires with accuracy especially at larger scales such as the national or even global scales [22]. However, burned area products developments can now be utilised as a valid source of fire contemporary fire history

information including the timing, frequency and progression of wildlife events for each month of the year across all land cover types.

Although, the MODIS fire data used in this study is freely available, regularly updated and provide repetitive coverage of fire prone landscapes [3, 16], it has some limitations. For example, MODIS fire data only starts from 2000 onwards which inhibits an extended analysis of burned areas before the year 2000 [22, 23]. In addition, unlike other sensors such as Synthetic Aperture Radar which can detect burned areas on cloudy days, the detection of burned areas by MODIS in different parts of the world can be affected by cloud cover and aerosols [22, 24]. Nevertheless, a recent comparison of four publicly available global burned area products revealed that MODIS Burned Area products and Fire CCI Burned Area Products from Medium Resolution Imaging Spectrometer (MERIS) perform better even in challenging conditions compared to other burned area products such as the Copernicus Burned Area Products [21]. Therefore, MODIS fire products can be relied on for the analysis of wildfire trends, spatial distribution and temporal distribution.

To improve our understanding of wildfire patterns in savannas, the aim of this study was to provide a long-term analysis of the spatial and temporal variations in burned areas using MODIS remotely sensed fire data from 2001 to 2020, with Zimbabwe used as a case study. Specifically, we sought to (i) examine the spatial variation in frequency of occurrence of burned areas over a twenty-year period; (ii) determine the drivers of spatial and temporal variations in burned areas in across Zimbabwe, and (iii) to examine differences in fire frequency between land cover types; (iv) to determine the validity of the MODIS burned area product data. It is anticipated that the results of this study will be useful in identifying spatial trends in fires, identify repeat or incidental fire areas and provide quantitative information for targeted fire management that will ultimately culminate in a fire forecasting system based on biophysical variables.

2. Materials and methods

2.1 Study area

The study was carried out in Zimbabwe, which is a landlocked country in southern Africa with a total area of 390,757 km². It is bordered by South Africa, Mozambique, Botswana and Zambia (Fig 1). The country is located between latitudes 15°30" and 22°30"S and longitudes 25°00" and 33°10"E. Altitude across the country varies from under 300m in the south-east to more than 2500m above mean sea level in the eastern parts. Annual rainfall varies from less than 400 mm in the southern and north-western parts of the country to above 1000 mm in the eastern mountainous areas [25, 26]. The mean annual rainfall in the country is 675 mm. There are two distinct seasons: wet and dry seasons. The wet season starts in November and ends in March, while the dry season begins in April and terminates in October. The mean monthly temperatures vary from 15°C in the winter months (June-July) to 24°C in the month of November, while average annual temperature ranges from 18°C in the eastern highlands of the country to 23°C in the Limpopo Valley [26]. These weather conditions support high biomass production in the central, northern, western and eastern parts of the country which provides fuel load for wildfire ignition and spread [10]. In Zimbabwe, the savanna ecosystem is characterized by a mixture of trees and tall grass which ensures abundant biomass fuel for fires particularly during the dry season. The country is under forests and woodlands, the savanna woodlands are made up of five woodland types which are: miombo, *Acacia species*, mopane, teak, and *Terminalia species* [8]. These woodlands consist of inter-mixed grasslands with woody plant cover which provides high biomass fuel that is required for fire ignition and spread.

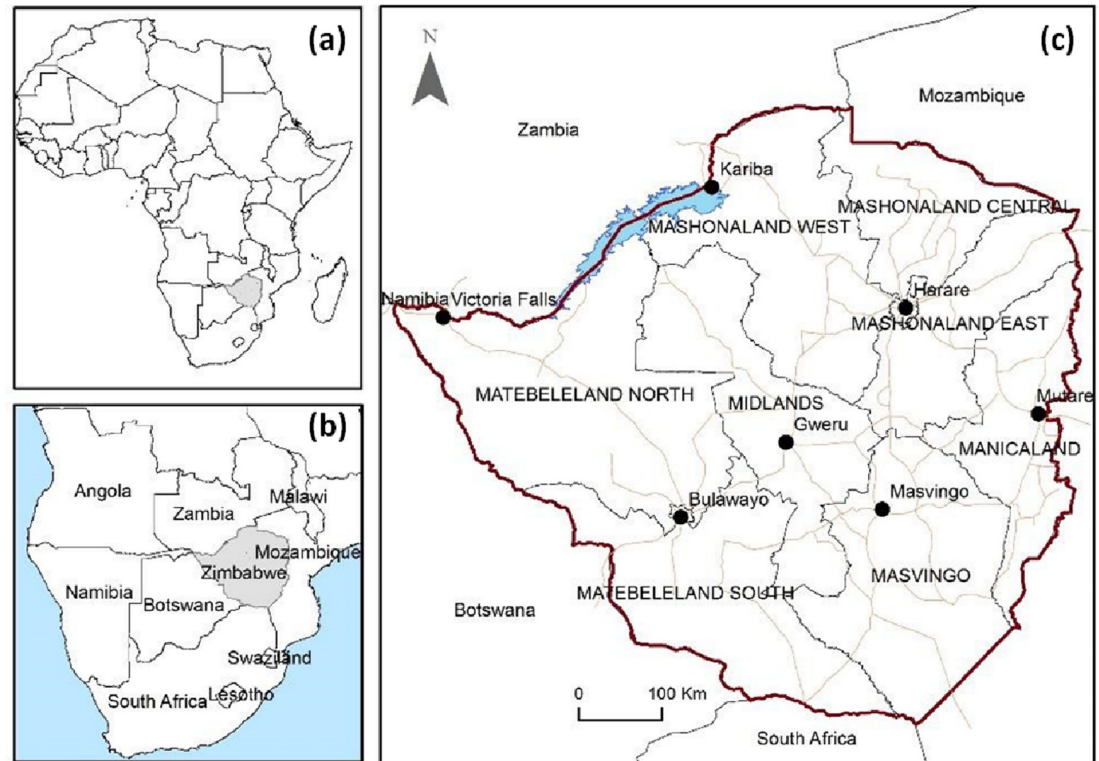


Fig 1. Location of Zimbabwe (c) the study area. The top insert (a) shows the location of Zimbabwe in Africa, and the bottom insert (b) shows the neighbouring countries of Zimbabwe in Southern Africa. (Shapefile data source: Department of Geography Geospatial Sciences and Earth Observation, University of Zimbabwe, 2022).

<https://doi.org/10.1371/journal.pclm.0000201.g001>

2.2 Data

2.2.1 Fire occurrence data. The fire data were derived from the Moderate Resolution Imaging Spectroradiometer (MODIS) Fire Climate Change Initiative Burned Area pixel product version 5.1. The portal was accessed via Google Earth Engine as an image collection (ESA/CCI/FireCCI/5_1). The product is available at global scale with a spatial resolution of 250m. The data considered in this study spanned from the 1st of January 2001 to the 1st of December 2020. Only burned pixels with a confidence level of $\geq 70\%$ were selected to ensure reliable fire data products [27]. The bidirectional reflectance model-based change detection algorithm was applied in the detection of fire pixels [27]. The algorithm uses spectral, temporal, and structural changes to detect burned areas at 250m grid cells. Burned pixels are characterised by deposits of charcoal and ash, removal of vegetation and alteration of the vegetation structure [22, 23, 27, 28]. The images are a series of pixels defined by a specific set of values i.e., Julian day of burning, water, unburned, snow and invalid data [23]. The pixels with values ranging from 1–366 which represented the Julian day burning and with other values such as 0 (the pixel is not burned), -1 (pixel is not observed in the month) and -2 (pixels that are not burnable: water bodies, bare areas, urban areas, permanent snow and ice) were considered in this study. The data uses the Julian dating system which is the continuous count of days from the beginning of the year to the end of the year.

2.2.2 Land use/cover data. ESA land cover data developed from Sentinel-2 imagery at a 20m resolution was downloaded from the following website: <http://2016africallandcover20m.esrin.esa.int/> and was used for determining the fire frequency and return intervals across

landcover types of Zimbabwe. We reclassified 19 ESA land cover categories into 9 based on similar vegetation structure and fuel composition, namely into: bare areas, bushland, cultivation, grassland, riverine vegetation, urban, water, wooded grassland, woodland, (Fig 2 and Table 1). These nine classes with similar vegetation structure, are commonly used by the Forestry Commission of Zimbabwe. The general descriptions of the different landcover classes are as given in Table 2:

2.2.3 Climate data. Climate data used for determining key climatic drivers of wildfire in different vegetation types were downloaded from the enhanced POWER Data Access Viewer (DAV) <https://power.larc.nasa.gov/data-access-viewer/>. The data was downloaded at daily time steps and summarised at both monthly and annual time steps. These variables included are specified in Table 3: temperature (T2M), specific humidity (weight of water vapor contained in a unit weight of air, QV2M), wind speed, maximum wind speed (WS2M_MAX) and minimum wind speed (WS2M_MIN), precipitation and root zone soil wetness (GWET-ROOT) (Table 3). The climate data were available at a spatial resolution of 0.5 * 0.625 degrees of latitude and longitude, respectively. The POWER solar data is based upon satellite observations from which surface insolation values are inferred [29] These satellite and model-based products have been shown to be sufficiently accurate to provide reliable solar and meteorological resource data over regions where surface measurements are sparse or non-existent [30]. In addition, the data is global and generally contiguous in time. The Meteorological parameters are derived from the NASA's GMAO MERRA-2 assimilation model and GEOS 5.12.4 FP-IT. MERRA-2 is a version of NASA's Goddard Earth Observing System (GEOS) Data Assimilation System [31]. The GEOS 5.12.4 data is processed by the POWER project team on a daily basis and appended to the end of the MERRA-2 daily time series to provide low latency products which are generally ready within about 2 days of real-time.

2.2.4 Vegetation Condition Index (VCI). The Vegetation Condition Index was calculated using MODIS normalized difference vegetation index (NDVI) data downloaded from <https://appears.earthdatacloud.nasa.gov>. The NDVI data were available as 16-day NDVI composites at a spatial resolution of 250m. The VCI compares the observed NDVI to the range of values observed in the same period in previous years. The VCI is expressed in % and gives an idea where the observed value is situated between the extreme values (minimum and maximum) in the previous years. Lower and higher values indicate bad and good vegetation state conditions, respectively.

$$VCI = \frac{NDVI_{cur} - NDVI_{min}}{NDVI_{max} - NDVI_{min}} \times 100 \quad (1)$$

Where:

$$NDVI = \frac{NIR - Red}{NIR + Red} \quad (2)$$

and for MODIS,

$$Red = \text{band 1}(620 - 670\text{nm}) \text{ and,}$$

$$NIR = \text{band 2}(841 - 876\text{nm})$$

To compute VCI, at first $NDVI_{min}$, $NDVI_{max}$ and $NDVI_{cur}$ need to be computed. $NDVI_{min}$ is defined as minimum value of NDVI in years (2001–2020). So, at first the minimum value of NDVI for each year is computed. $NDVI_{max}$ is defined as maximum value of NDVI in years (2001–2020) and $NDVI_{cur}$ is the mean NDVI for the current year.

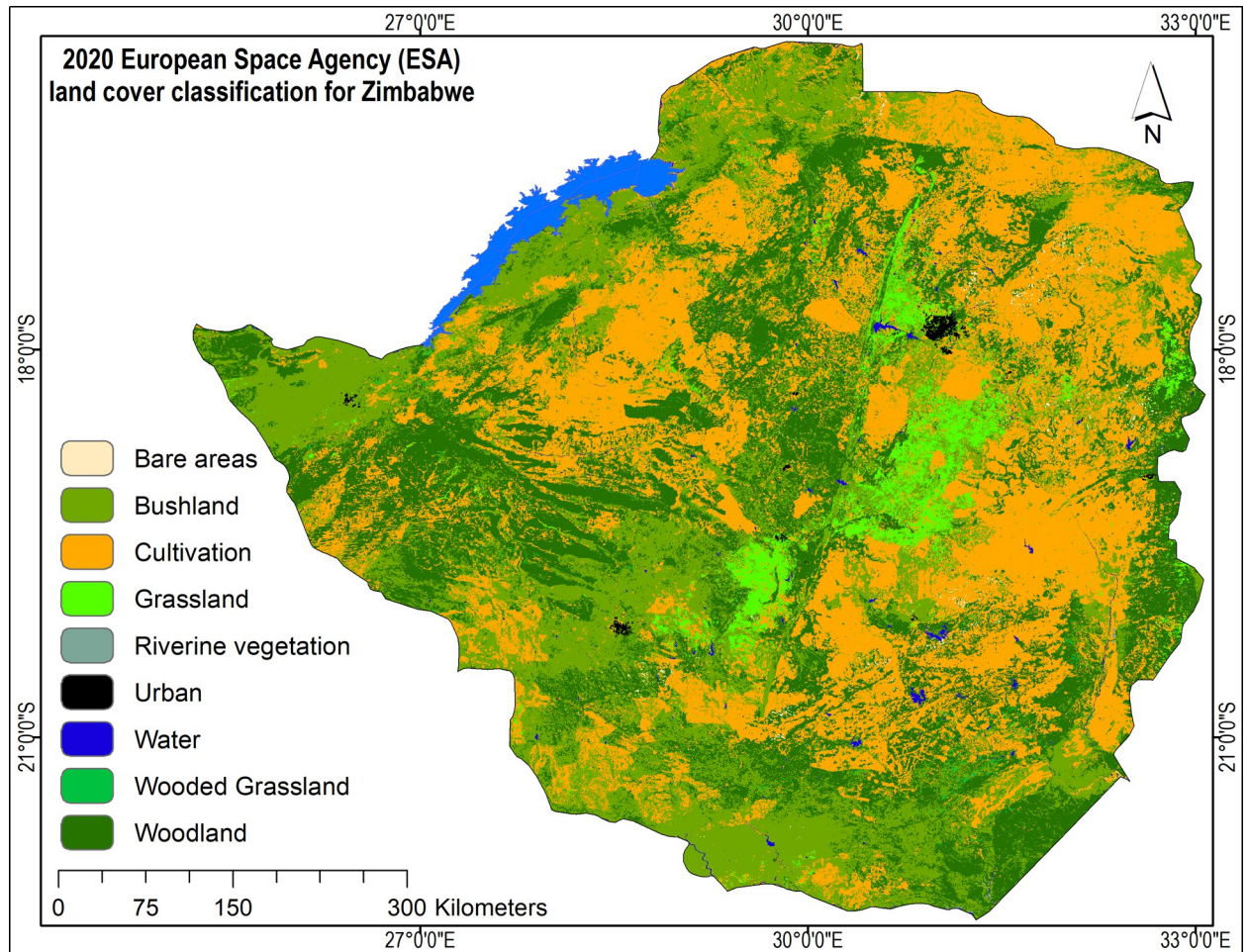


Fig 2. The 2020 European Space Agency (ESA) land cover data developed from Sentinel-2 imagery for Zimbabwe. (Data source: ESA. Land Cover CCI Product User Guide Version 2. Tech. Rep. (2017). Available at: maps.elie.ucl.ac.be/CCI/viewer/download/ESACCI-LC-Ph2-PUGv2_2.0.pdf).

<https://doi.org/10.1371/journal.pclm.0000201.g002>

2.3 Data processing and analysis

Burned areas extracted from raw images were reclassified into 2 classes: burned areas (1) and unburned areas (0) in ArcGIS 10.8 (<https://desktop.arcgis.com/en>). From the binary map, overall monthly fire frequency was derived by summing all the images with fire in that month from the first to the last year. For example, to get fire frequency for the month of December, all fire images for the month of December from 2001 to 2020 were summed in ArcGIS 10.8 software (<https://desktop.arcgis.com/en>). Similarly, to calculate yearly fire frequency map all classified burned area images of each year from January to December were summed. The frequency indicated the number of times each pixel was burned over the respective months and years for the ~20-year period. The final monthly and annual fire frequency maps were produced using ArcGIS 10.8 software. To determine the fire frequency per landcover class, an overlay analysis was performed using the Sentinel 2016 landcover map (European Space Agency Climate Change Initiative—Land Cover project 2017) over the 20-year period. Kruskal Wallis statistic was applied in R statistical software (R version 4.1.2) to test whether frequency of burned areas significantly differed across different landcover types in Zimbabwe. In

Table 1. Reclassification of the ESA vegetation classes into classes used in this paper.

Value	ESA Vegetation Classes	Reclassified Vegetation Classes
1	cropland rainfed	Cultivation
2	cropland rainfed herbaceous cover	Cultivation
3	cropland rainfed tree or shrub cover	Cultivation
4	cropland irrigated	Cultivation
5	mosaic cropland	Cultivation
6	mosaic natural vegetation	Woodland
7	tree broadleaved evergreen closed to open	Woodland
8	tree broadleaved deciduous closed to open	Woodland
9	tree broadleaved deciduous closed	Woodland
10	tree broadleaved deciduous open	Woodland
11	mosaic tree and shrub	Bushland
12	mosaic herbaceous	Bushland
13	shrubland	Bushland
14	shrubland deciduous	Wooded Grassland
15	grassland	Grassland
16	sparse vegetation	Bushland
17	tree cover flooded fresh or brackish water	Riverine vegetation
18	tree cover flooded saline water	Riverine vegetation
19	shrub or herbaceous cover flooded	Riverine vegetation
20	urban	Urban / Built-up
21	bare areas	Bare areas
22	water	Water

<https://doi.org/10.1371/journal.pclm.0000201.t001>

Table 2. General Description of the different vegetation types in Zimbabwe.

Value	Class	Description
1	Woodland	This is a broad class which can be defined as open to dense stand of indigenous trees with a canopy cover of 20–80% and tree height is between 5 and 15m. The crowns of the adjacent trees are often touching but not densely interlocking. Frequently the trees are widely spaced and are deciduous or semi-deciduous
2	Wooded Grassland	Opened to closed shrubs and bushes (height less than 5m) in which proportion of trees must not exceed the proportion of the shrubs. These areas predominantly vegetated with grasses and the trees cover ranges between 5 to 10% of the area. This is characterised by clumped or scattered trees or bushes 1–15 m high and with a canopy cover of 2–20%. Bush and tree clumps are usually found on termite mounds
3	Grassland	In this class is trees are very scattered or virtually absent. The canopy cover of existing trees/bushes constitute 2%. Grassland is usually associated with areas that are seasonally waterlogged and shallow soils that preclude the establishment of tree species.
4	Cultivated areas	Cultivation refers to land where the major land use is agricultural crop production. In this class most of the natural vegetation has been removed. Most cultivated areas especially in communal lands are characterised by scattered residual trees left on contour ridges, around gardens and homesteads.
5	Riverine Vegetation	Regularly flooded areas which can be covered by grasses, shrubs and trees
6	Bushland	Sparsely vegetated areas, made up of indigenous woody cover with a canopy closure of 20–80% and height 1–5m. Bushland differs from woodland in the height. Bushes are usually multi-stemmed and trees are localised in clumps or are widely scattered.
7	Bare areas	Areas without vegetation or almost no vegetation such as rocks, and barren soil
8	Built up areas	Artificial surfaces, settlements and industrial areas, built up areas and airstrips
9	Water bodies	Areas that are covered with water all-season

<https://doi.org/10.1371/journal.pclm.0000201.t002>

Table 3. Variables used in for determining key climatic drivers of wildfire in different vegetation types.

Variable	Description
T2M	Temperature at 2 Meters (C)
T2M_MIN	Minimum Temperature at 2 Meters (C)
T2M_MAX	Maximum Temperature at 2 Meters (C)
GWETROOT	Root zone soil wetness
QV2M	Specific Humidity at 2 Meters (g/kg)
T2M_RANGE	Temperature Range at 2 Meters (C)
WS10M	Wind Speed at 10 Meters (m/s)
WS10M_MAX	Maximum Wind Speed at 10 Meters (m/s)
WS2M_MIN	Minimum wind speed at 10 Meters (m/s)
T2M_MAX	Maximum Temperature at 2 Meters (C)
PRECTOT	Precipitation (mm day-1)

<https://doi.org/10.1371/journal.pclm.0000201.t003>

addition, piecewise regression was implemented in R statistical software (R version 4.1.2) (R Core Team 2021) to determine changes in annual burned area trends at 95% confidence interval.

2.4 Validation of burned area data

Data used for validating the model were obtained from the Environmental Management Agency of Zimbabwe. The data were collected by district officers of the agency as part of the environmental data they gather in their routine work. Once a fire is detected, district officers collect information that include coordinates where fire occurred and an estimate of areal extent of burned areas. The point data collected in the field were overlaid with the burned area derived from the satellite imagery. The field data were characterised by lack of consistency hence only points for the year 2019 which were proportionately higher ($n = 34$) fire occurrence were considered. The overall accuracy ($\text{True Positive} + \text{True Negative} / (\text{Positive} + \text{Negative})$) and F1 score ($2 * \text{True Positive} / (2 * \text{True Positive} + \text{False Positive} + \text{False Negative})$) were calculated by dividing the number of times when there was agreement between satellite derived burned area and ground data from the confusion matrix of the matching of MODIS fire and the reference data. True positive is when data from the satellites predict a fire that was observed on the ground, while the A true negative result is a correct satellite determination that no fire exist. False positive and false negative occur when the satellite detects a fire that is absent and fails to detect a fire that is actually on the ground, respectively. The approach was necessitated by the fact that fire data were available as presence only data.

2.5 Modelling the drivers of burned areas

In this study, Generalized Linear Model (GLM) was used to predict burned area as a function of climatic variables. The GLM generalizes linear regression by allowing the linear model to be related to the response variable via a link function and allowing the magnitude of the variance of each measurement to be a function of its predicted value [32]. It unifies various other statistical models, including linear regression, logistic regression, and poisson regression [32, 33]. GLM is a flexible generalization of ordinary linear regression. Variables were first tested for collinearity using a variance inflation factor of 10 based on thresholds suggested in literature [5, 34]. The uncorrelated variables were incorporated in a model (for forward selection) using the stepAIC function (R MASS package version 7.3–58.3) (Venables and Ripley, 2002) implemented using R statistical software version 4.1.2 (R Core Team 2021). This process yielded a

set of models arranged by AIC. Based on the AIC results, the model with the lowest AIC was selected as the best model that predicted burned area in the country. For the analysis we also included lagged version of a time series, shifting the time base back by n years to understand the individual and cumulative effects of preceding years on the fire occurrence. Our hypothesis was that the biophysical characteristics of n preceding years may affect fire severity and extent in the following years and can be modelled from the GLM as lagged variables.

3. Results

3.1 Dynamics of burned areas across Zimbabwe from 2000 to 2019

The MODIS burned area data had an overall accuracy of 0.69 and F1 Score of 0.81 suggesting a relatively high fire detection of fire by the MODIS Sensor. Burned area markedly increased every year for 10 years and declined yearly thereafter. The largest burned areas were recorded in 2010 and 2011 (Fig 3) during which a total of 58,081km² (15%) and 61,330km² (16%) of land was burned in different parts of the country, respectively. Over, the 20-year period, an average of 40,086.56 km² (11%) of land was burned annually in the country. Burned area increased from 3,689 km² in 2001 to 61,330km² in 2011 and decreased thereafter reaching its lowest extent in 2020 (1,161km²).

Spatially, several areas in Zimbabwe had a marked decrease in fire occurrence between the years 2000–2010 and 2011–2021. For example, (a) areas around Gonarezhou in Chiredzi district located in the South East of the country; (b) areas around Bulawayo; (c) areas around Chikomba district in the central part of the country and (d) areas in the northern parts of the country around Hurungwe and Kariba Districts; all showed a marked decrease in both the fire frequency and the spatial extent of burned areas (Fig 4).

An analysis of average monthly burned area from 2001 to 2020 shows that rainfall months had the least burned area particularly November to April (Fig 5). During this period a minimum average of 7 km² and a maximum average of 1,1 km² in burned area were recorded.

Burned area decreased considerably towards the end of the rainfall season (May) with the maximum burned area recorded in the driest of months of the year i.e., June to October. This relatively dry period coincides with the fire season in the country.

3.2 Spatial variations in wildfire frequency

Fire frequency i.e., the number of times a pixel burned, varied markedly across the country over the 20-year period (Fig 6). Most of the fire activity was concentrated in the central, northern, and north-western parts of Zimbabwe. Notable areas that experienced persistent and frequent fires include areas around Chinhoyi, Banket, Mhangura, Kariba, Hwange, Shamnva and around Chivhu. The greater parts of these areas recorded fire frequency of greater than 7 suggesting that these pixels burned more than 7 times over the 20-year period. In contrast, the eastern, southern, and western parts of the country experienced the least fire frequency with either no burned area recorded, or having burned only once.

3.3 Fire frequency by vegetation type based on Sentinel vegetation classification

Fire frequency significantly (Kruskal-Wallis $\chi^2 = 7346.3$, $df = 7$, p -value = 0.000) varied across vegetation types with (Table 4). Grassland and tree cover area had the second and third most frequency of burned areas. Wooded grassland and cultivated areas had the least frequency of burned areas. In all vegetation types, fire frequency ranged from zero to 20 suggesting that some areas never burned at all while others burn nearly every year (Fig 7).

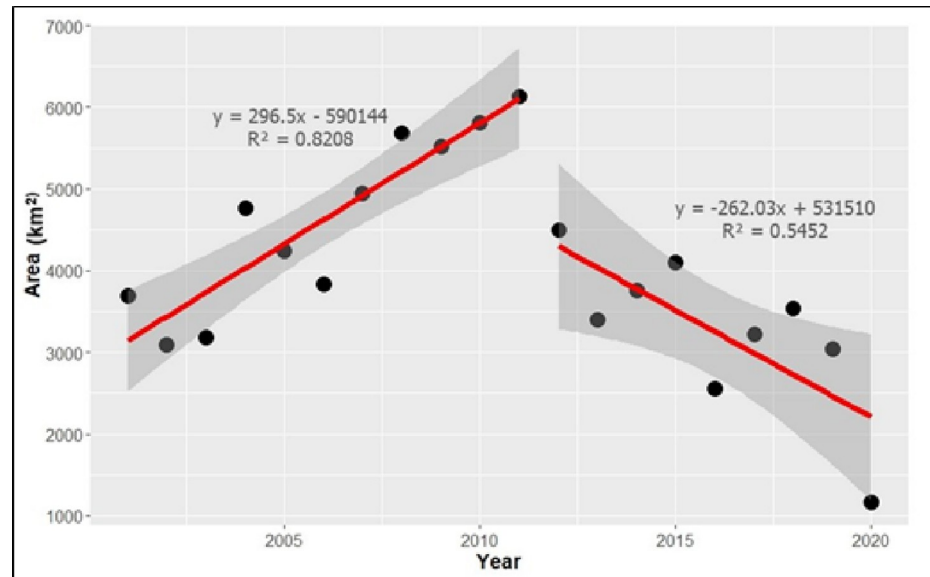


Fig 3. Temporal changes in burned areas across Zimbabwe from the year 2001 to 2020. A positive trend in burned area is observed from 2001 up to 2011 while a negative trend is observed thereafter.

<https://doi.org/10.1371/journal.pclm.0000201.g003>

In terms of extent, bushland had the highest mean burned area (2.8) all the vegetation type while riverine vegetation was the least burned area (0.7). Over the 20 years, 57.2% of the country did not experience any fires (Table 5), whilst only 11% of the country was burned at least once, and 1.2% was burned at least 10 times, with 0.01% being burned at least 20 times. Thus, areas which were burned for more than 10 times over the 20 years would be targeted and prioritised for fire control and mitigation measures (Table 5 and Fig 6).

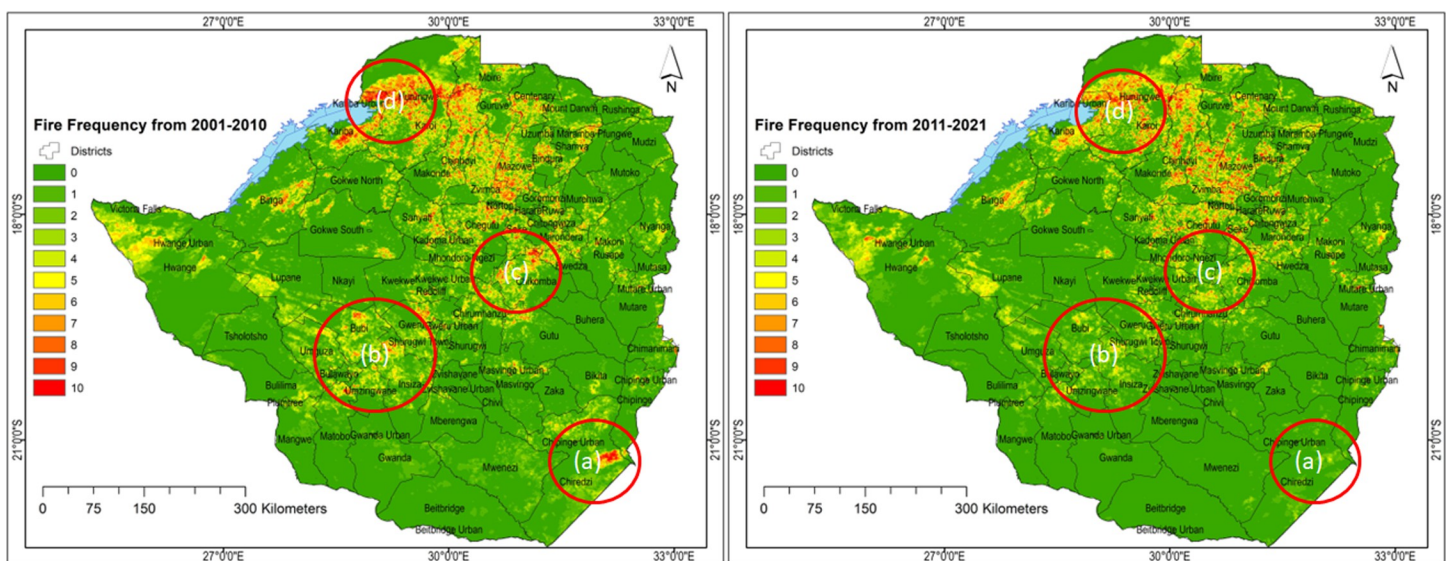


Fig 4. Notable decrease in burned areas in Zimbabwe between the decades 2001–2010 and 2011 to 2021. (Data source: Roteta, E., et al. (2019) Development of a Sentinel-2 burned area algorithm: Generation of a small fire database for sub-Saharan Africa. <https://doi.org/10.1016/j.rse.2018.12.011>).

<https://doi.org/10.1371/journal.pclm.0000201.g004>

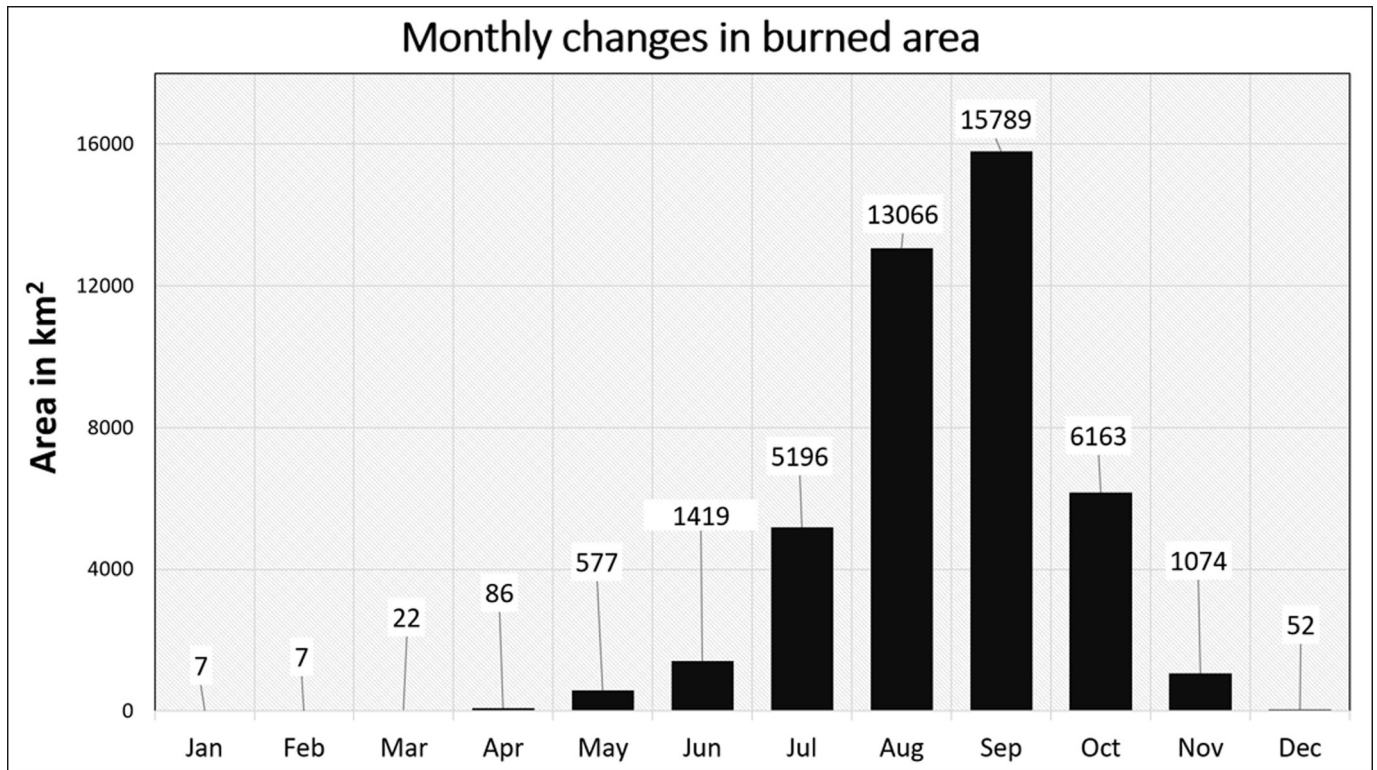


Fig 5. Monthly changes in average burned area in Zimbabwe between 2001 and 2020 to show the peak and low periods of fire extent. (Data source: European Space Agency MODIS fire product).

<https://doi.org/10.1371/journal.pclm.0000201.g005>

3.4 Climatic drivers of spatial and temporal variations in burned areas between 2000 and 2020

The resultant model contained precipitation, vegetation condition index, temperature at 2m, specific humidity at 2 meters (QV2M), wind speed at 2 meters (WS2M), maximum wind speed at 2 meters (WS2M_MAX) and minimum wind speed at 2 meters (WS2M_MIN). Results of the relationship between burned areas and changes in climate variables show that temperature, windspeed and root zone soil wetness significantly influenced the extent of burned areas in Zimbabwe over the 20 years period (Table 6). Specifically, temperature and windspeed positively influenced burned areas while Root zone soil wetness had the opposite effect. Of these climate variables, root zone soil wetness had the greatest effect.

It was observed that burned area positively responds to preceding four-year rainfall with a 1mm increase resulting in a thirty-eighty-fold increase in burned area (Fig 8). The annual average rainfall received between 2001 and 2020 ranged from 430 recorded in 2006 to and 876 observed in 2004. On the other hand, minimum burned area (11,610,000ha) was recorded in 2020 after the second lowest rainfall amount recorded in 2019.

4. Discussion

The main objective of this study was to analyse spatial and temporal trends in the distribution of wildfires in Zimbabwe using MODIS remote sensing data. The study provides three contributions that are important in ecosystem and land management in that it (i) analyses the long-term changes in fire regimes, spatial destruction and extent, (ii) provides a country-scale

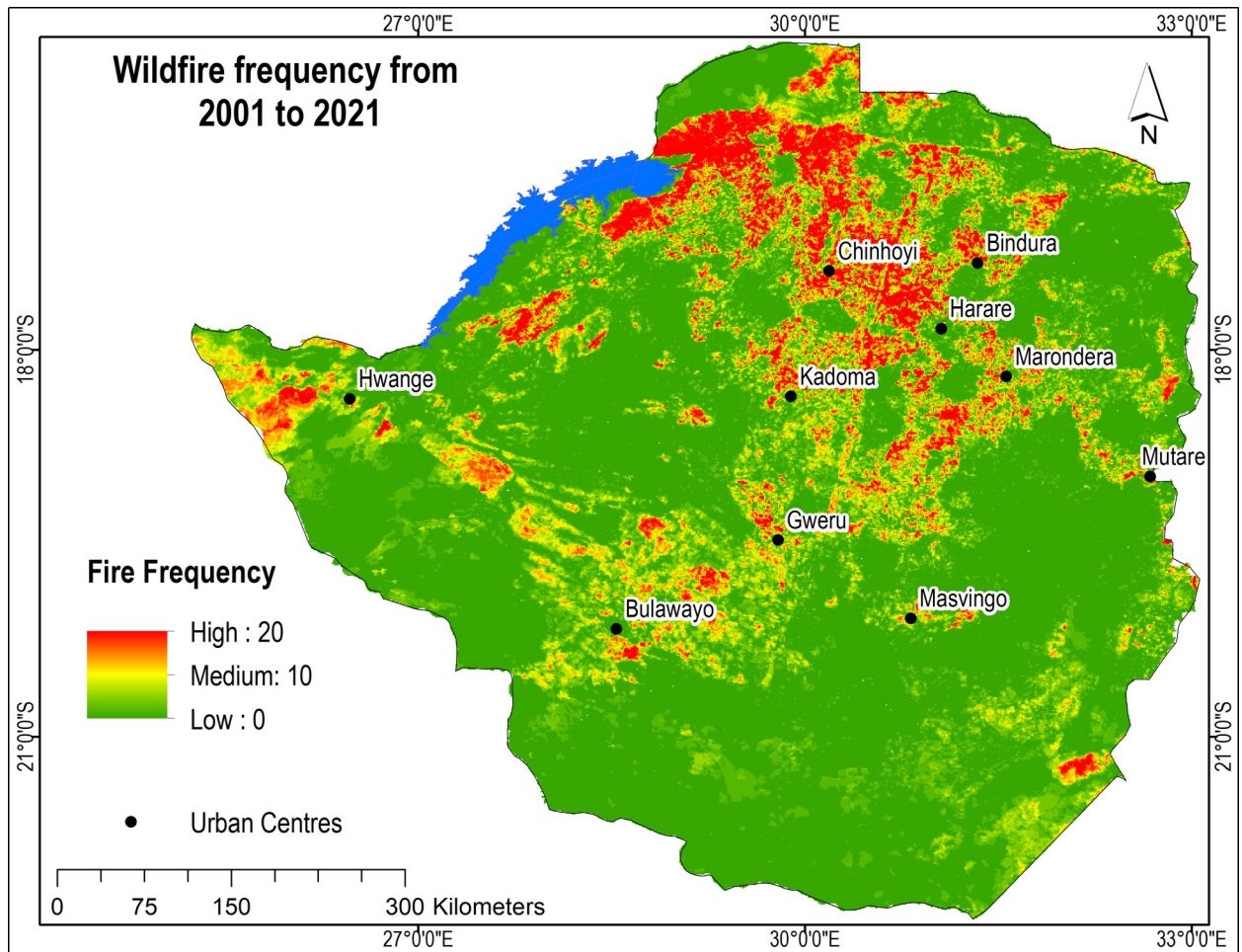


Fig 6. Spatial and temporal variation in wildfire frequency from January 2001 to December 2020. (Data source: Roteta, E., et al. (2019) Development of a Sentinel-2 burned area algorithm: Generation of a small fire database for sub-Saharan Africa. <https://doi.org/10.1016/j.rse.2018.12.011>).

<https://doi.org/10.1371/journal.pclm.0000201.g006>

assessment of fire impacts over time and (iii) presents an innovative method for continuous fire assessment that can be upscaled or transferred to other areas for fire trend and impact monitoring. This information is not only important for the understanding of biophysical

Table 4. Vegetation classes, total area occupied and the respective fire frequency within each vegetation type.

Landcover Type	Area km ²	% of Area	Fire Frequency				
			Min	Max	Range	Mean	Std
Riverine Vegetation	475	0.12%	0	9	9	0.7	1.0
Bare areas	159	0.04%	0	12	12	1.0	2.2
Built up areas	631	0.16%	0	12	12	0.7	1.7
Cultivated areas	104063	26.63%	0	19	19	1.6	3.2
Woodland	86648	22.17%	0	20	20	2.3	3.5
Grassland	68539	17.54%	0	20	20	2.6	4.0
Wooded Grassland	126539	32.38%	0	20	20	1.7	2.9
Bushland	381	0.10%	0	18	18	2.8	4.1
Open Water	3321	0.85%	0	18	18	0.4	1.5

<https://doi.org/10.1371/journal.pclm.0000201.t004>

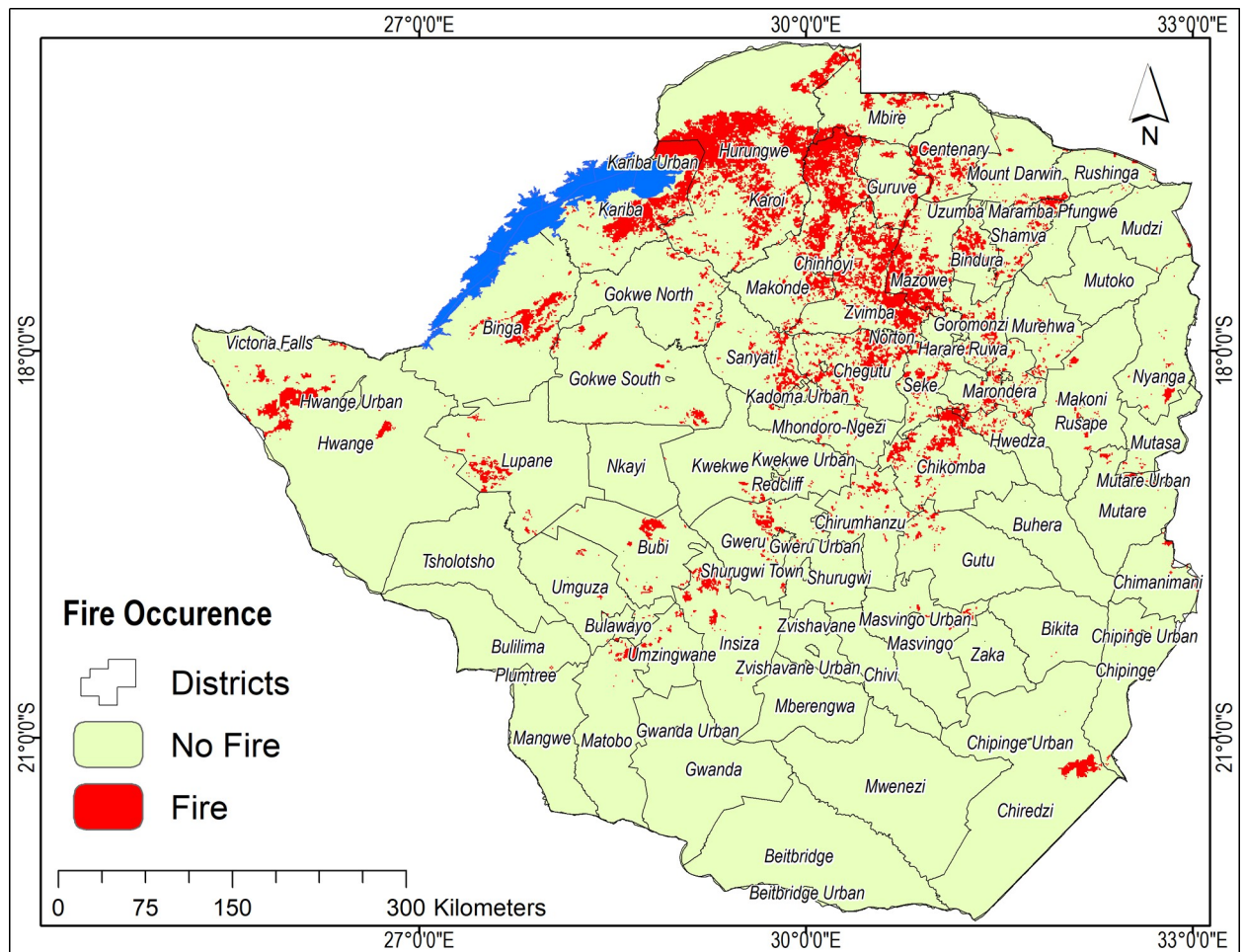


Fig 7. Districts in Zimbabwe affected by fires (every year for at 10-year period or more—in red) from 2001 to 2020. (Data source: Roteta, E., et al. (2019) Development of a Sentinel-2 burned area algorithm: Generation of a small fire database for sub-Saharan Africa. <https://doi.org/10.1016/j.rse.2018.12.011>).

<https://doi.org/10.1371/journal.pclm.0000201.g007>

drivers of fire extent and severity but also identifies fire-hotspot areas that need attention and more focused monitoring for managing fire events and spread. It is expected that the results of this study are important for management of landscapes and ecosystems in the context of changing climate at regional level.

The results indicate significant spatial and temporal variation in burned areas across savanna ecosystems of Zimbabwe over the past twenty years. We find a noteworthy increase in the frequency and coverage of burned areas from June to October in the northern, central, western, and south-eastern parts of the country. This period coincides with the dry season and therefore biomass that would have accumulated during the wet season will have dried up thereby providing fuel load for fire ignition. The result is not surprising as previous studies in southern Africa identified the predominance of wildfire during this prolonged dry period. High temperatures and dry matter which can be easily ignited are the major factors leading to an increase in fire incidence during the dry season [28]. However, as the rain season starts, the occurrence and spatial extent of wildfires decreases drastically across the country with limited fire activity observed in the western and southern parts of the country. Changes in weather conditions are the main drivers of decline in fire activity particularly high moisture content in

Table 5. Percentage of area versus fire frequency from 2001 to 2020 in Zimbabwe.

Fire Frequency	Percentage of area burned over the 20 years
0	57.2%
1	11.4%
2	6.7%
3	4.8%
4	3.8%
5	3.0%
6	2.5%
7	2.1%
8	1.8%
9	1.5%
10	1.2%
11	1.0%
12	0.8%
13	0.7%
14	0.5%
15	0.4%
16	0.3%
17	0.2%
18	0.1%
19	0.03%
20	0.01%

<https://doi.org/10.1371/journal.pclm.0000201.t005>

vegetation and soil, and high humidity which reduce ignition and extent of fires in the ecosystem [35]. The identification of temporal windows during which fires dominate provides range-land managers with accurate timeframes during which allocation of resources for managing wildfires could be prioritised.

An important result from this study is that over the 20-year period fire hotspots were concentrated in specific districts and vegetation types in the northern and western regions of the country i.e., Hurungwe, Makonde, Kariba, Hwange, Zvimba, Mazowe, and Chegutu. In terms of vegetation, the most burned areas occurred within wooded grassland and cultivated areas while the least burned area was recorded in sparsely vegetated areas. Recent studies have shown that agricultural activities such as burning of crop residues and land clearing through logging and burning felled trees are the main causes of wildfires in these districts which are predominantly resettlement or communal lands where agriculture is dominant [14, 18].

Table 6. Climatic variables explaining variations in burned area with variables in bold being significant.

Variable	Standard Error	T-value	P-value
Intercept	255513.4	4.370	0.001
Precipitation	15.9	-1.327	0.211
Vegetation Condition	303.0	1.494	0.163
Temperature (2m)	9316.5	3.857	0.002
QV2M	11881.6	1.546	0.150
WS2M	24458.9	3.338	0.007
GWETROOT	216265.8	-4.066	0.002
WS2M_MAX	4308.4	1.972	0.074
WS2M_MIN	108709.5	1.089	0.299

<https://doi.org/10.1371/journal.pclm.0000201.t006>

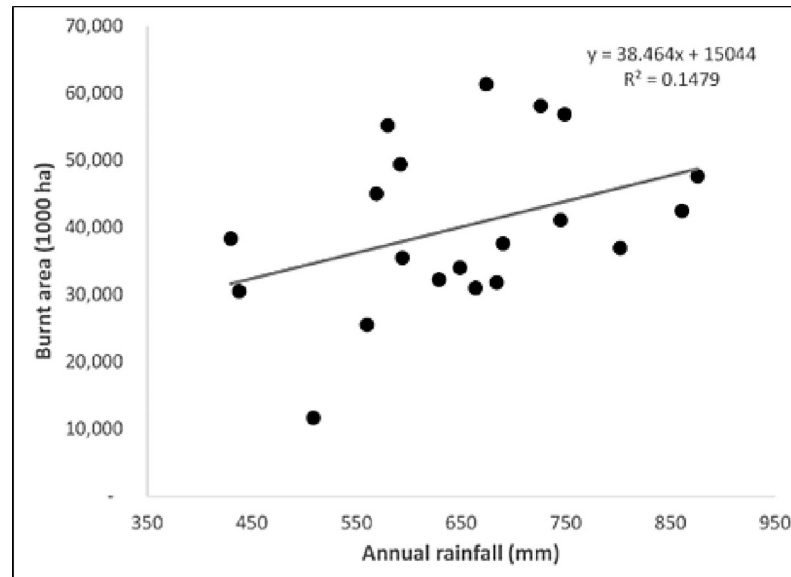


Fig 8. Relationship between mean annual rainfall over the preceding four years and total burned area across Zimbabwe between 2001 and 2020.

<https://doi.org/10.1371/journal.pclm.0000201.g008>

In addition, high atmospheric temperatures, slope, humidity, fuel load and other anthropogenic activities are also key drivers of fires in these districts as reported by [36] as well. In contrast, districts in the southern and eastern parts of the country experienced the least wildfires over the study period. Although the mechanisms explaining low fire frequency during the study period were not tested, low biomass or sparse vegetation could explain this observation. The southern parts of the country receive the least amount of rainfall and support less biomass production thereby limiting fuel load resulting in fewer fires compared to the rest of the country [10, 36]. In addition, the change in climate (rising temperatures and reduced rainfall) as noted by [37] could explain the reduced biomass in these areas. The spatially varying nature of fires in the country could guide fire management by focusing limited resources in areas that are in greatest need i.e., districts with high frequency than elsewhere.

This study has shown that burned areas increased from 2001 to 2011 before decreasing thereafter (Figs 3 and 4). Noteworthy is that the increasing trend in fires during the first decade post the year 2000 coincides with the Fast Track Land Reform Programme (FTLRP) [16]. The FTLRP led to population increase, land clearing and hunting using fires by resettled farmers which increased not only fire ignition but spread as well [8, 16]. Results of this study have shown a general decreasing trend in burned areas after 2011 which could be attributable to the introduction of fire control measures by the Environmental Management Agency of Zimbabwe. The control measures included awareness campaigns, formation of fire teams, implementation of wide firebreaks and annual fire awareness promotions in the whole country but information on the changes in extent and reach of these is not available [16]. Therefore, basing on our findings, more research on the trends, outreach methods and reach of fire campaign methods is required. The decreasing trend in burned area identified in this study aligns with previous studies that have reported this phenomenon at various spatial scales such as global and continental scale Africa [38, 39]. Therefore, the approach adopted here could be used to assess the effectiveness of interventions on wildfires such as legislation and wildfire management systems.

Results of this study indicated that root zone soil wetness (soil moisture) was the most important variable that negatively influenced variations in burned areas. The negative effect of soil moisture on burned areas suggests a decrease in burned areas with increase in soil moisture content. The result is not surprising as soil moisture has been previously identified as an important determinant of wildfire hazard on ecosystems and landscapes across the globe [40–42]. In the context of wildfires, soil moisture does not only influence fuel load through controls on primary productivity but also through determining fuel load moisture content and subsequent flammability [43]. In fact, high rainfall years are associated with elevated soil moisture availability thereby promoting primary productivity, a key ingredient for fires [44, 45]. Ultimately, soil moisture mediates preheating and ignition of unburned fuels, rate of fire spread as well as radiative power of fires [46]. However, the influence of soil moisture on wildfire has been shown to be a function of climate. For example, [47] report that above average soil moisture supports high biomass accumulation capable of supporting large fires while in humid regions dry soil moisture conditions precedes wildfires through creating conducive environment for fire ignition and flammability.

In Zimbabwe, the southern and western parts of the country receive the least amounts of rainfall, thereby limiting the amount of fuel load to support meaningful fire activity. In contrast, the eastern parts of the country are the most humid (>1000mm annual rainfall) and support the highest woody primary productivity in the country. Rainfall in the eastern highlands is spread across almost all months of the year implying that the region could be too humid to burn, and the regular rainfall episodes experienced in the region rewets the fuel load. However, the predominantly humid conditions, low herbaceous understory alongside low temperatures retard fire ignition and flammability. The northern parts of the country receive intermediate annual rainfall, high temperatures and relatively high herbaceous primary productivity thereby supporting high wildfire activity. Thus, our results are in line with the classical hump shaped fire-aridity aridity relationship [48–50] in which fuel load limits fire activity in very arid conditions, while dry and humid conditions limit fire activity in wet regions with well-developed vegetation.

Of the variables considered in this study, temperature and wind speed emerged as the second and third most important variables explaining burned area variability, respectively. The two variables are critical determinants of ignition conditions with wind considered as the most critical as it desiccates fuel load as well as determining the trajectory of the fire front. Together with relative humidity (inferred from the soil moisture), these variables have been widely incorporated in prescribed fire management [51]. For example, humidity is used as a fire control measure for prescribed burning and wildfire suppression [52, 53].

A key observation from this study is the positive but lagged response of burned area to preceding four-year annual rainfall with a 1 mm increase inducing close to a forty-fold increase in burned area. Although the relationship between antecedent rainfall and total area burned in any given year is well established [44, 45], results from this study are surprising in terms of the time scale. Unlike previous studies that have reported lagged responses of between one and two years, this study demonstrated that a four-year time lag in preceding annual rainfall better predicts burned area in Zimbabwe than other time scales. While the mechanism explaining this observation was not tested, the four-year time lag suggests that the greater part of the country does not have sufficient fuel to support fire ignition and spread at shorter time scales, thus a four-year time scale provide optimal period for fuelwood accumulation.

Fire size and occurrence has been evaluated previously by various scholars, although they focused on smaller spatial scales for example a single district which confines understanding of fire occurrence at a larger scale. This study is among the first to characterise spatial and temporal wildfire patterns at the national scale and at relatively longer temporal window (2 decades)

thereby providing wildfire managers with an opportunity to prioritise resource allocation aimed in the control of fire. Furthermore, key drivers of burned area dynamics were determined thereby providing ecological basis for wildfire management in predominantly savanna landscapes of Zimbabwe. Thus, this study has not only generated new insights into wildfire evolution in the country but has also demonstrated dynamics in the spatial configuration of burned patches in the landscape. These results further amplify the importance of freely available remotely sensed data and accompanying geo-technologies in wildfire monitoring and management. Although we are confident that we robustly identified the biophysical drivers of fire risk and severity in Zimbabwe, we are aware to the fact that fires are also driven by human behaviour as influenced by socioeconomic factors that cannot be captured by this type of modelling. Therefore, further research weighing the contribution of biophysical factors and socio-economic/behavioural factors is recommended especially in the identified fire hotspot areas.

5. Conclusion

This study used burned area MODIS data to characterise wildfire frequency as well as spatial configuration of burned areas over a 20-year period across savanna ecosystems of Zimbabwe. Results indicated that there is high frequency of wildfires in Zimbabwe with some parts recording as high as 20 fire incidences over the two decades. In addition, the study showed that soil moisture, temperature and wind speed are the key drivers of wildfire in savanna landscapes of Zimbabwe. The study has shown that the integration of remotely sensed fire data within a spatially analytical framework can provide useful insights into fire evolution that can be used to guide wildfire control and management in fire prone ecosystems. Moreover, resource allocation for fire management and mitigation can be optimised through targeting areas most affected by wildfires especially during the dry season where wildfire activity is at its peak.

Supporting information

S1 Data. T2M, MERRA-2 Temperature at 2 Meters (C). QV2M, MERRA-2 Specific Humidity at 2 Meters (g/kg). RH2M, MERRA-2 Relative Humidity at 2 Meters (%). WS2M, MERRA-2 Wind Speed at 2 Meters (m/s). GWETTOP, MERRA-2 Surface Soil Wetness (1). T2M_MAX, MERRA-2 Temperature at 2 Meters Maximum (C). T2M_MIN, MERRA-2 Temperature at 2 Meters Minimum (C). GWETROOT, MERRA-2 Root Zone Soil Wetness (1). WS2M_MAX, MERRA-2 Wind Speed at 2 Meters Maximum (m/s). WS2M_MIN, MERRA-2 Wind Speed at 2 Meters Minimum (m/s). PRECTOTCORR, MERRA-2 Precipitation Corrected (mm/day). (XLSX)

Author Contributions

Conceptualization: Munyaradzi Davis Shekede, Samuel Kusangaya.

Data curation: Courage B. Chavava, Isaiah Gwitira, Abel Chemura.

Formal analysis: Munyaradzi Davis Shekede, Courage B. Chavava, Abel Chemura.

Methodology: Munyaradzi Davis Shekede, Samuel Kusangaya, Isaiah Gwitira, Abel Chemura.

Writing – original draft: Munyaradzi Davis Shekede, Samuel Kusangaya, Courage B. Chavava, Isaiah Gwitira.

Writing – review & editing: Samuel Kusangaya.

References

1. Scholes RJ, Archer SR. Tree-Glass Interactions in Savannas. *Annual Review of Ecology and Systematics*, Vol. 28 (1997), pp. 517–544. URL: <http://www.jstor.org/stable/2952503>.
2. Richards SA, Possingham HP, Tizard J. Optimal Fire Management for Maintaining Community Diversity. *Wiley on behalf of the Ecological Society of America*. URL: <https://www.jstor.org/stable/2641336> *Ecol*. 2023; 9: 880–892.
3. Magadzire N. Reconstruction of a fire regime using MODIS burned area data: Charara Safari Area, Zimbabwe. Stellenbosch University. 2013.
4. Kosoe EA, Osumanu IK, Barnes VR. Wildfire Management in the Tain II Forest Reserve of Ghana: An Evaluation of Community Participation. *OALib*. 2015; 02: 1–11. <https://doi.org/10.4236/oalib.1101964>
5. Shekede MD, Murwira A, Masocha M, Gwitira I. Spatial distribution of *Vachellia karoo* in Zimbabwean savannas (southern Africa) under a changing climate. *Ecol Res*. 2018; 33: 1181–1191. <https://doi.org/10.1007/s11284-018-1636-7>
6. Govender N, Trollope WSW, Van Wilgen BW. The effect of fire season, fire frequency, rainfall and management on fire intensity in savanna vegetation in South Africa. *Journal of Applied Ecology*. 2006; 43: 748–758. <https://doi.org/10.1111/j.1365-2664.2006.01184.x>
7. Lasslop G, Coppola AI, Voulgarakis A, Yue C, Veraverbeke S. Influence of Fire on the Carbon Cycle and Climate. *Curr Clim Change Rep*. 2019; 5: 112–123. <https://doi.org/10.1007/s40641-019-00128-9>
8. Nyamadzawo G, Gwenzi W, Kanda A, Kundhlande A, Masona C. Understanding the causes, socio-economic and environmental impacts, and management of veld fires in tropical Zimbabwe. *Fire Sci Rev*. 2013; 2: 2. <https://doi.org/10.1186/2193-0414-2-2>
9. WWF. *Fire Management Manual: Wildlife Management Series*. WWF Harare; 2001.
10. Anyamba A, Justice CO, Tucker CJ, Mahoney R. Seasonal to interannual variability of vegetation and fires at SAFARI 2000 sites inferred from advanced very high-resolution radiometer time series data. *Journal of Geophysical Research: Atmospheres*. 2003; 108. <https://doi.org/10.1029/2002jd002464>
11. Levin N, Heimowitz A. Mapping spatial and temporal patterns of Mediterranean wildfires from MODIS. *Remote Sens Environ*. 2012; 126: 12–26. <https://doi.org/10.1016/j.rse.2012.08.003>
12. Shekede MD, Gwitira I, Mamvura C. Spatial modelling of wildfire hotspots and their key drivers across districts of Zimbabwe, Southern Africa. *Geocarto Int*. 2021; 36: 874–887. <https://doi.org/10.1080/10106049.2019.1629642>
13. Phiri M, Zingwena S, Mahamba SM. Community based fire management; experiences from the FAO funded project in the provinces of Manicaland and Matabeleland north, Zimbabwe 5. 5th International Wildland Fire Conference. 2011; 1–10.
14. Chinamatira L, Mtetwa S, Nyamadzawo G. Causes of wildland fires, associated socio-economic impacts and challenges with policing, in Chakari resettlement area, Kadoma, Zimbabwe. *Fire Sci Rev*. 2016; 5: 1–11. <https://doi.org/10.1186/s40038-016-0010-5>
15. Wokekoro E. The Impact of Forest Fires on Property Values and the Environment. *International Journal of Research in Applied, Natural and Social Sciences*. 2020; 8: 51–62. Available: www.impactjournals.us
16. Maponga R, Ahmed F, Mushore TD. Remote sensing-based assessment of veld fire trends in multiple interwoven land tenure systems in Zimbabwe. *Geocarto Int*. 2018; 33: 612–626. <https://doi.org/10.1080/10106049.2017.1289557>
17. Kusangaya S, Sithole V. Remote sensing-based fire frequency mapping in a savannah rangeland. *South African Journal of Geomatics*. 2015; 4: 36. <https://doi.org/10.4314/sajg.v4i1.3>
18. Mpakairi KS, Tagwireyi P, Ndaimani H, Madiri HT. Distribution of wildland fires and possible hotspots for the Zimbabwean component of Kavango-Zambezi Transfrontier Conservation Area. *South African Geographical Journal*. 2019; 101: 110–120. <https://doi.org/10.1080/03736245.2018.1541023>
19. Zhang Y, Lim S, Sharples JJ. Modelling spatial patterns of wildfire occurrence in South-Eastern Australia. *Geomatics, Natural Hazards and Risk*. 2016; 7: 1800–1815. <https://doi.org/10.1080/19475705.2016.1155501>
20. Masocha M, Dube T, Mpofo NT, Chimunhu S. Accuracy assessment of MODIS active fire products in southern African savannah woodlands. *Afr J Ecol*. 2018; 56: 563–571. <https://doi.org/10.1111/aje.12494>
21. Humber ML, Boschetti L, Giglio L, Justice CO. Spatial and temporal intercomparison of four global burned area products. *Int J Digit Earth*. 2019; 12: 460–484. <https://doi.org/10.1080/17538947.2018.1433727> PMID: 30319711
22. Roy DP, Boschetti L, Justice CO, Ju J. The collection 5 MODIS burned area product—Global evaluation by comparison with the MODIS active fire product. *Remote Sens Environ*. 2008; 112: 3690–3707. <https://doi.org/10.1016/j.rse.2008.05.013>

23. Giglio L, Boschetti L, Roy D, Hoffman A, Humber M. Collection 6 MODIS Burned Area product User Guide Versión 1.3. Nasa. 2020; 1–26. Available: https://lpdaac.usgs.gov/documents/875/MCD64_User_Guide_V6.pdf
24. Lasko K. Incorporating Sentinel-1 SAR imagery with the MODIS MCD64A1 burned area product to improve burn date estimates and reduce burn date uncertainty in wildland fire mapping. *Geocarto Int.* 2021; 36: 340–360. <https://doi.org/10.1080/10106049.2019.1608592>
25. Gwitira I, Murwira A, Zengeya FM, Masocha M, Mutambu S. Modelled habitat suitability of a malaria causing vector (*Anopheles arabiensis*) relates well with human malaria incidences in Zimbabwe. *Applied Geography.* 2015; 60: 130–138. <https://doi.org/10.1016/j.apgeog.2015.03.010>
26. Manatsa D, Mushore TD, Gwitira I, Sakala LC, Ali LH, Chemura A, et al. Revision of Zimbabwe's Agro-Ecological Zones. Harare; 2020.
27. Boschetti L, Roy D, Hoffmann AA, Humber M. MODIS Collection 5 Burned Area Product MCD45. User Guide. 2008;Version 1.: 1–12.
28. Roy DP, Lewis PE, Justice CO. Burned area mapping using multi-temporal moderate spatial resolution data—a bi-directional reflectance model-based expectation approach. *Remote Sens Environ.* 2002; 83: 263–286. [https://doi.org/10.1016/S0034-4257\(02\)00077-9](https://doi.org/10.1016/S0034-4257(02)00077-9)
29. White JW, Hoogenboom G, Wilkens PW, Stackhouse PW, Hoel JM. Evaluation of satellite-based, modelled-derived daily solar radiation data for the continental United States. *Agron J.* 2011; 103: 1242–1251. <https://doi.org/10.2134/agronj2011.0038>
30. Bai J, Chen X, Dobermann A, Yang H, Cassman KG, Zhang F. Evaluation of nasa satellite-and model-derived weather data for simulation of maize yield potential in China. *Agron J.* 2010; 102: 9–16. <https://doi.org/10.2134/agronj2009.0085>
31. Bosilovich MG, Robertson FR, Takacs L, Molod A, Mocko D. Atmospheric water balance and variability in the MERRA-2 reanalysis. *J Clim.* 2017; 30: 1177–1196. <https://doi.org/10.1175/JCLI-D-16-0338.1>
32. Zhao Y, Cen Y. Data Mining Applications with R. Data Mining Applications with R. Academic Press; 2013. <https://doi.org/10.1016/C2012-0-00333-X>
33. Zhao Y, Miner SD. Data Mining Applications with R: ProQuest Tech Books. 2014. Available: <http://proquest.safaribooksonline.com.proxy1.library.mcgill.ca/book/programming/r/9780124115118>
34. Sulaiman MS, Abood MM, Sinnakaudan SK, Shukor MR, You GQ, Chung XZ. Assessing and solving multicollinearity in sediment transport prediction models using principal component analysis. *ISH Journal of Hydraulic Engineering.* 2021; 27: 343–353. <https://doi.org/10.1080/09715010.2019.1653799>
35. Chen Y, Morton DC, Jin Y, Gollatz GJ, Kasibhatla PS, Van Der Werf GR, et al. Long-term trends and interannual variability of forest, savanna and agricultural fires in South America. *Carbon Manag.* 2013; 4: 617–638. <https://doi.org/10.4155/cmt.13.61>
36. Chingono TT, Mbohwa C. Fire hazard modelling in southern Africa. *Lecture Notes in Engineering and Computer Science.* 2015; 2219: 514–519.
37. Kusangaya S, Warburton ML, Archer van Garderen E, Jewitt GPW. Impacts of climate change on water resources in southern Africa: A review. *Physics and Chemistry of the Earth.* 2014;67–69: 47–54. <https://doi.org/10.1016/j.pce.2013.09.014>
38. Andela N, Morton DC, Giglio L, Chen Y, Van Der Werf GR, Kasibhatla PS, et al. A human-driven decline in global burned area. *Science (1979).* 2017; 356: 1356–1362. <https://doi.org/10.1126/science.aal4108> PMID: 28663495
39. Earl N, Simmonds I. Spatial and Temporal Variability and Trends in 2001–2016 Global Fire Activity. *Journal of Geophysical Research: Atmospheres.* 2018; 123: 2524–2536. <https://doi.org/10.1002/2017JD027749>
40. Krueger ES, Ochsner TE, Engle DM, Carlson JD, Twidwell D, Fuhlendorf SD. Soil Moisture Affects Growing-Season Wildfire Size in the Southern Great Plains. *Soil Science Society of America Journal.* 2015; 79: 1567–1576. <https://doi.org/10.2136/sssaj2015.01.0041>
41. O S, Xinyuan H, Rene O. Observational evidence of wildfire-promoting soil moisture anomalies. *Sci Rep.* 2020; 10. <https://doi.org/10.1038/s41598-020-67530-4> PMID: 32620812
42. Kavhu B, Ndaimani H. Analysing factors influencing fire frequency in Hwange National Park. *South African Geographical Journal.* 2022; 104: 177–192. <https://doi.org/10.1080/03736245.2021.1941219>
43. Kreye JK, Kane JM, Varner JM, Hiers JK. Radiant heating rapidly increases litter flammability through impacts on fuel moisture. *Fire Ecology.* 2020; 16. <https://doi.org/10.1186/s42408-020-0067-3>
44. Van Wilgen BW, Govender N, Biggs HC, Ntsala D, Funda XN. Response of savanna fire regimes to changing fire-management policies in a large African National Park. *Conservation Biology.* 2004; 18: 1533–1540. <https://doi.org/10.1111/j.1523-1739.2004.00362.x>

45. Archibald S, Roy DP, van Wilgen BW, Scholes RJ. What limits fire? An examination of drivers of burnt area in Southern Africa. *Glob Chang Biol.* 2009; 15: 613–630. <https://doi.org/10.1111/j.1365-2486.2008.01754.x>
46. Msweli ST, Potts AJ, Fritz H, Kraaij T. Fire weather effects on flammability of indigenous and invasive alien plants in coastal fynbos and thicket shrublands (Cape Floristic Region). *PeerJ.* 2020; 8. <https://doi.org/10.7717/peerj.10161> PMID: 33240598
47. Zubkova M, Giglio L, Humber ML, Hall J V., Ellicott E. Conflict and climate: Drivers of fire activity in Syria in the twenty-first century. *Earth Interact.* 2021; 25: 119–135. <https://doi.org/10.1175/EI-D-21-0009.1>
48. Krawchuk MA, Moritz MA, Krawchuk MA, Moritz MA. Constraints on global fire activity vary across a resource gradient. *Ecological Society of America.* 2018; 92: 121–132.
49. Pausas JG, Paula S. Fuel shapes the fire-climate relationship: Evidence from Mediterranean ecosystems. *Global Ecology and Biogeography.* 2012; 21: 1074–1082. <https://doi.org/10.1111/j.1466-8238.2012.00769.x>
50. Duane A, Castellnou M, Brotons L. Towards a comprehensive look at global drivers of novel extreme wildfire events. *Clim Change.* 2021; 165: 1–21. <https://doi.org/10.1007/s10584-021-03066-4>
51. Nieman WA, Van Wilgen BW, Leslie AJ. A review of fire management practices in African savanna-protected areas. *Koedoe.* 2021; 63: 1655. <https://doi.org/10.4102/koedoe.v63i1.1655>
52. Fernandes PM, Botelho HS. A review of prescribed burning effectiveness in fire hazard reduction. *Int J Wildland Fire.* 2003; 12: 117–128. <https://doi.org/10.1071/WF02042>
53. Morgan GW, Tolhurst KG, Poynter MW, Cooper N, McGuffog T, Ryan R, et al. Prescribed burning in south-eastern Australia: history and future directions. *Aust For.* 2020; 83: 4–28. <https://doi.org/10.1080/00049158.2020.1739883>